Original Article | Thoracic Imaging

eISSN 2005-8330
https://doi.org/10.3348/kjr.2019.0789
Korean J Radiol 2020;21(6):756-763

Check for updates

Korean Journal of Radiology
KJR

Optimal Attenuation Threshold for Quantifying CT Pulmonary Vascular Volume Ratio

Hyun Woo Goo, MD, PhD, Sang Hyub Park, RT, BD

All authors: Department of Radiology and Research Institute of Radiology, University of Ulsan College of Medicine, Asan Medical Center, Seoul, Korea

Objective: To evaluate the effects of attenuation threshold on CT pulmonary vascular volume ratios in children and young adults with congenital heart disease, and to suggest an optimal attenuation threshold.

Materials and Methods: CT percentages of right pulmonary vascular volume were compared and correlated with percentages calculated from nuclear medicine right lung perfusion in 52 patients with congenital heart disease. The selected patients had undergone electrocardiography-synchronized cardiothoracic CT and lung perfusion scintigraphy within a 1-year interval, but not interim surgical or transcatheter intervention. The percentages of CT right pulmonary vascular volumes were calculated with fixed (80–600 Hounsfield units [HU]) and adaptive thresholds (average pulmonary artery enhancement [PA_{avg}] divided by 2.50, 2.00, 1.75, 1.63, 1.50, and 1.25). The optimal threshold exhibited the smallest mean difference, the lowest *p*-value in statistically significant paired comparisons, and the highest Pearson correlation coefficient.

Results: The PA_{avg} value was 529.5 ± 164.8 HU (range, 250.1–956.6 HU). Results showed that fixed thresholds in the range of 320–400 HU, and adaptive thresholds of PA_{avg}/1.75–1.50 were optimal for quantifying CT pulmonary vascular volume ratios. The optimal thresholds demonstrated a small mean difference of ≤ 5%, no significant difference (> 0.2 for fixed thresholds, and > 0.5 for adaptive thresholds), and a high correlation coefficient (0.93 for fixed thresholds, and 0.91 for adaptive thresholds).

Conclusion: The optimal fixed and adaptive thresholds for quantifying CT pulmonary vascular volume ratios appeared equally useful. However, when considering a wide range of PAavg, application of optimal adaptive thresholds may be more suitable than fixed thresholds in actual clinical practice.

Keywords: *Cardiothoracic CT; Congenital heart disease; CT volumetry; Lung perfusion scintigraphy; Optimal threshold; Pulmonary vessels*

INTRODUCTION

In patients with cyanotic congenital heart disease and peripheral pulmonary stenosis, cardiothoracic computed tomography (CT) is commonly used for the evaluation of pulmonary artery morphology, a necessity for treatment planning and post-treatment surveillance (1, 2). Lung perfusion scintigraphy has been useful for assessing the differential right-to-left lung perfusion ratio, which is also essential in these patients (3, 4). However, cardiothoracic CT had not been utilized to quantify pulmonary vascularity until recent studies demonstrated it could be applied to evaluate the pulmonary vascular volume ratio, in addition to pulmonary artery anatomy (5-7). Nonetheless, these studies demonstrated that confounding factors such as pulmonary vascular obstruction and pulmonary regurgitation increased CT measurement errors (5). CT measurements are also substantially influenced by the cardiac phase, and therefore, acquisition of cardiothoracic CT data at the end-systolic phase is recommended (6).

Additionally, the optimal attenuation threshold should be used to achieve a better result for threshold-based quantification (8-14). A threshold-based segmentation approach is also used to quantify CT pulmonary vascular volume ratios; therefore attenuation thresholds for

Received: October 21, 2019 **Revised:** November 21, 2019
Accepted: January 21, 2020
Corresponding author: Hyun Woo Goo, MD, PhD, Department of Radiology and Research Institute of Radiology, University of Ulsan College of Medicine, Asan Medical Center, 88 Olympic-ro 43-gil, Songpa-gu, Seoul 05505, Korea.
• Tel: (822) 3010-4388 • Fax: (822) 476-0090
• E-mail: ghw68@hanmail.net
This is an Open Access article distributed under the terms of the Creative Commons Attribution Non-Commercial License (https://creativecommons.org/licenses/by-nc/4.0) which permits unrestricted non-commercial use, distribution, and reproduction in any medium, provided the original work is properly cited.

Copyright © 2020 The Korean Society of Radiology

Korean Journal of Radiology
KJR

quantification may influence results (5-7). However, the ratio may not significantly change despite different attenuation thresholds when the degree of pulmonary vascular enhancement is similar on both sides. To date, attenuation threshold effects on CT pulmonary vascular volume ratios have not been systemically assessed. Consequently, the objectives of this study were to evaluate the effects of attenuation threshold on CT pulmonary vascular volume ratios in children and young adults with congenital heart disease, and to suggest optimal attenuation thresholds.

MATERIALS AND METHODS

Our Institutional Review Board approved this retrospective study and waived the requirement for informed consent.

Study Population

The study subjects included 52 consecutive children and young adults (median age, 4 years; age range, 2 months to 28 years; 31 male patients) with congenital heart disease between January 2011 and December 2016, who underwent: 1) cardiothoracic CT examination acquired at the end-systolic phase, and 2) lung perfusion scintigraphy within a 1 year-interval (median, 60 days; range, 0–361 days), but not interim surgical or transcatheter interventions. The same study population was previously used to evaluate the clinical value of CT pulmonary vascular volume ratios (5). The majority of the patients (71.2%, 37/52) were either repaired tetralogy of Fallot (n = 27), or repaired pulmonary atresia (n = 10). The study population also had a history of surgical pulmonary artery angioplasty (n = 21), pulmonary artery stent placement (n = 4), and balloon pulmonary artery angioplasty (n = 3).

Cardiothoracic CT

A second-generation dual-source CT scanner (SOMATOM Definition Flash; Siemens Healthineers, Forchheim, Germany) was used to acquire electrocardiography (ECG)-synchronized scans from the thoracic inlet to the first lumbar vertebra in 2 x 64 x 0.6 mm slices. The z-flying focal spot technique with a 0.75-mm slice width and a 0.4-mm reconstruction interval were used. Depending on patient age and cooperation, prospectively ECG-triggered sequential scanning with additional respiratory triggering was performed in 34 free-breathing sedated patients, single breath-hold retrospectively ECG-gated spiral scanning was performed in 17 non-sedated patients, and prospectively ECG-triggered high-pitch spiral scanning was performed in one free-breathing sedated patient. Oral chloral hydrate (50 mg/kg) was initially used to sedate the patients, and intravenous midazolam (0.1 mg/kg) or ketamine (1 mg/kg) was additionally administered as required. As previously described, an additional respiratory gating system (AZ-733V; Anzai Medical Co. Ltd., Tokyo, Japan) was utilized for combined prospective ECG and respiratory triggering to minimize respiratory motions in free-breathing children (15, 16). CT protocols were optimized with the following parameters to minimize radiation dose and maintain diagnostic image quality: 1) centering the patient in the CT gantry isocenter, 2) using combined tube current modulation (CARE Dose 4D; Siemens Healthineers), 3) entering the individual body size-adapted radiation dose before scan range adjustment, 4) using an aggressive version of the ECG-controlled tube current modulation (MinDose; Siemens Healthineers), 5) using a biphasic chest pain protocol for the retrospectively ECG-gated spiral scan, and 6) using sinogram-affirmed iterative reconstruction (SAFIRE; Siemens Healthineers) (17-23). An optimized triphasic or quadriphasic injection protocol developed at our institution was used to maximize uniform cardiovascular enhancement, and minimize peri-venous streak artifacts from undiluted contrast agent. This protocol involved an iodinated contrast agent (iomeprol; Iomeron 400, 400 mg I/mL; Bracco Imaging SpA, Milan, Italy; 1.5–2.0 mL/kg) injected at a rate of 0.5–3.0 mL/s, and a bolus-tracking technique determined scan delay, with a 150 Hounsfield units (HU) trigger threshold in the left ventricular cavity.

CT Pulmonary Vascular Volumetry

CT pulmonary vascular volumetry was performed on a commercially available workstation (Advantage Workstation 4.6; GE Healthcare, Milwaukee, WI, USA). After the bony thorax was removed, an attenuation threshold of 80 HU was applied to isolate the thoracic cardiovascular structures from other soft tissues, and the resulting CT data were saved (Fig. 1A). The CT data corresponding to the central section were extracted from the overall thoracic cardiovascular structure data by eliminating peripheral section data at the pulmonary artery bifurcation, and the atrial-pulmonary venous junctions (Fig. 1B). The right and left pulmonary vessels (Fig. 1C) were segmented by subtraction of the central section from the entire thoracic cardiovascular structures. Stents were excluded from pulmonary vessels

 https://doi.org/10.3348/kjr.2019.0789

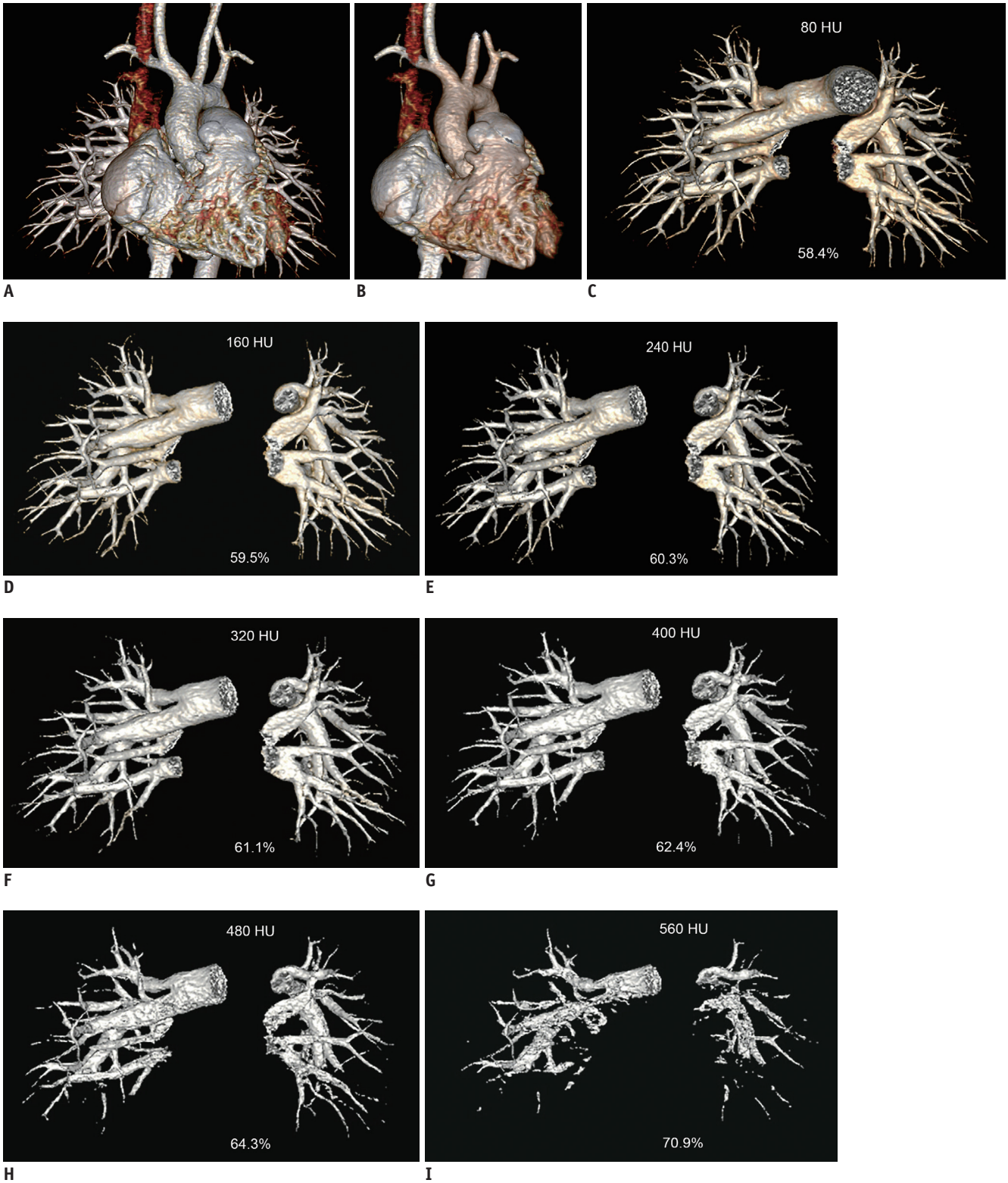

Fig. 1. 4-year-old girl with repaired left pulmonary artery sling.
A-C. Frontal volume-rendered CT images showing thoracic cardiovascular structures segmented by applying lowest attenuation threshold of 80 HU **(A)**, volume after exclusion of branch pulmonary arteries and pulmonary veins **(B)**, and pulmonary vascular volumes obtained by subtracting central section from entire cardiovascular structure **(C)**. **D-I.** Additional attenuation thresholds were applied to pulmonary vascular volumes by serially increasing value by 40 HU, up to 600 HU. **C-I.** Quantified percentage of CT right pulmonary vascular volume was gradually increased from 58.4% at 80 HU to 70.9% at 560 HU. HU = Hounsfield units

https://doi.org/10.3348/kjr.2019.0789

Korean Journal of Radiology
KJR

in four patients with pulmonary artery stents by applying an attenuation threshold of 800 HU. The segmented right and left pulmonary vessel volumes were calculated with the workstation "volumetry" menu. An approximate post-processing time of 15 minutes was required for each patient.

Fixed Attenuation Threshold

Attenuation thresholds were serially increased from 80 HU to 600 HU in 40 HU increments to determine the optimal fixed threshold (Fig. 1C-I). We used a wide threshold range based on visually determined attenuation thresholds (120–160 HU) reported in a previous study, to avoid missing the optimal fixed threshold (1).

Adaptive Attenuation Threshold

The average pulmonary artery enhancement (PA_{avg}) was calculated from the right and left branch pulmonary arterial enhancement values measured by placing a round region of interest in the central half of the branch pulmonary artery. Next, adaptive attenuation thresholds were individually calculated by dividing PA_{avg} with 2.50 (PA_{avg}/2.50), 2.00 (PA_{avg}/2.00), 1.75 (PA_{avg}/1.75), 1.63 (PA_{avg}/1.63), 1.50 (PA_{avg}/1.50), and 1.25 (PA_{avg}/1.25), respectively.

Lung Perfusion Scintigraphy

After intravenous injection with a body surface area-indexed percentage of the standard 80 MBq adult dose of technetium-99m macroaggregated albumin, lung perfusion scintigraphy was performed with a gamma camera. Pulmonary blood flow was reflected by the distribution of radioactivity in the lungs. Lung fields were viewed in anterior and posterior planes, and the relative perfusion percentage was calculated with geometric mean counts for each lung (Fig. 1C). The right lung perfusion percentage determined by lung perfusion scintigraphy was regarded as the reference standard to determine the optimal attenuation threshold for quantifying the CT right pulmonary vascular volume percentage.

Statistical Analysis

Statistical analyses were performed with Excel (Microsoft Corp., Redmond, WA, USA). Continuous variables were expressed as the mean ± standard deviations or median with range, and categorical variables were expressed as frequency with percentage. The right pulmonary vascular volume percentages measured by cardiothoracic CT, and the right lung perfusion percentages measured by lung perfusion scintigraphy for each threshold were compared and correlated with the paired *t* test and the Pearson correlation coefficient. A *p*-value of less than 0.05 was considered statistically significant. In addition, absolute differences between the two values were calculated and averaged. The optimal threshold definition for the CT pulmonary vascular volume ratio included: 1) the smallest mean absolute difference (≤ 5.0%), 2) the lowest statistically significant difference (*p*-value) compared to the reference values measured by lung perfusion scintigraphy, and 3) the highest Pearson correlation coefficient.

RESULTS

The right lung perfusion percentage value measured with lung perfusion scintigraphy was 69.1 ± 15.0%. The CT right pulmonary vascular volume percentages determined with fixed thresholds were relatively stable in all patients from 80 HU to 400 HU, but began to show substantial fluctuations in some patients from 440 HU to 600 HU (Fig. 2). The mean CT right pulmonary vascular volume percentages determined with the fixed thresholds were initially 65.8% at 80 HU, and gradually increased and peaked to 70.4% at 440 HU (Table 1). The values were significantly lower than the right lung perfusion percentages measured with perfusion scintigraphy in the 80–200 HU range ($p < 0.02$), but no significant differences were found in the 240–600 HU range ($p > 0.05$) (Table 1). The mean absolute difference between the two imaging modalities was less than 5.0% in the 160–400 HU range (Table 1). High Pearson correlation coefficients ($R = 0.93$) were found in the 80–400 HU range, and subsequently gradually decreased at fixed thresholds greater than 440 HU (Table 1). Consequently, 320 HU, 360 HU, and 400 HU fixed attenuation thresholds were regarded as optimal for CT pulmonary vascular volume ratio calculations.

The mean pulmonary artery enhancement value was 529.5 ± 164.8 HU (range, 250.1–956.6 HU). The mean CT right pulmonary vascular volume percentages determined with adaptive thresholds were initially 67.2% at PA_{avg}/2.50, and gradually increased and peaked at 71.1% at PA_{avg}/1.25 (Table 2). Only the values observed at PA_{avg}/2.50 were significantly lower than the right lung perfusion percentages measured with lung perfusion scintigraphy ($p < 0.03$), and other values showed no significant differences ($p > 0.05$) (Table 2). The mean absolute difference between

 https://doi.org/10.3348/kjr.2019.0789

the two imaging modalities was less than 5.0% for all adaptive thresholds, except for $PA_{avg}/1.25$ (Table 2). Pearson correlation coefficients were high (R = 0.91–0.92) for all adaptive thresholds (Table 2). Therefore, $PA_{avg}/1.75$, $PA_{avg}/1.63$, and $PA_{avg}/1.50$ were determined as optimal among the six different adaptive thresholds for calculating

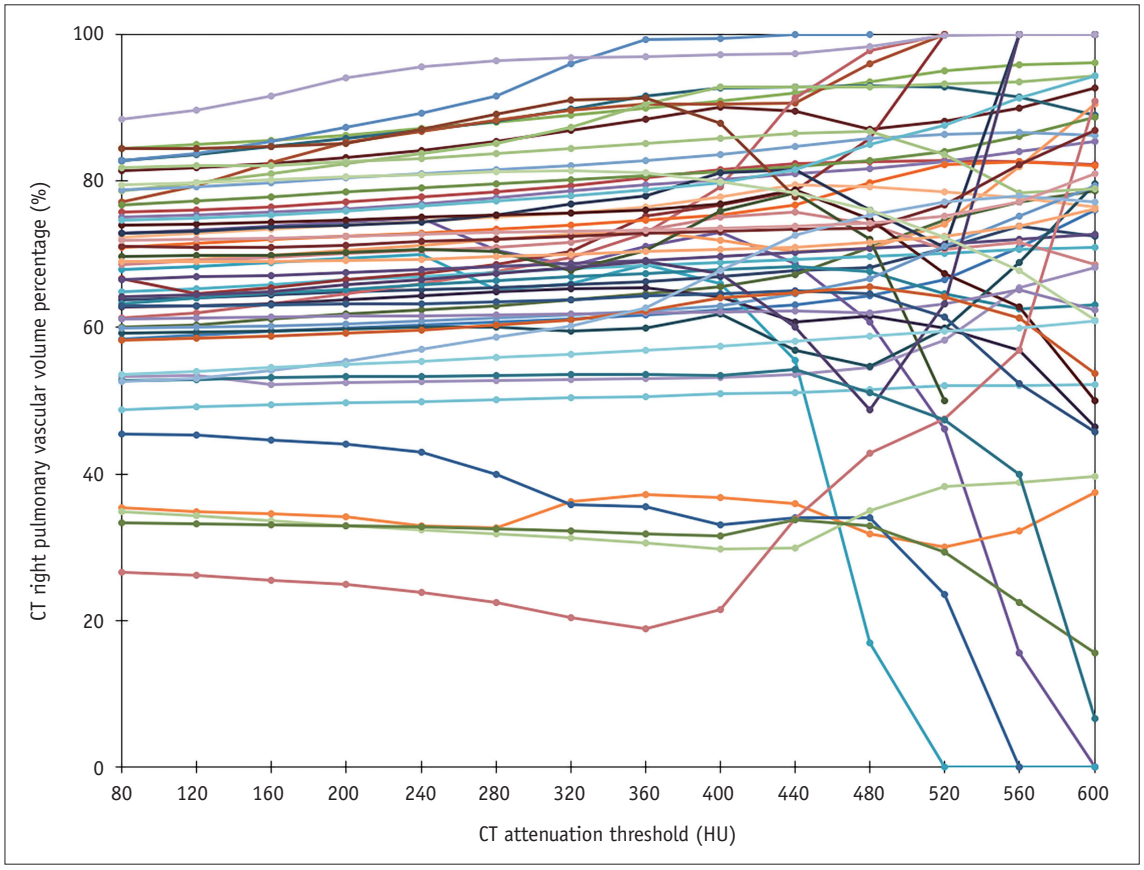

Fig. 2. Graphical illustration of changes in percent of CT right pulmonary vascular volume with fixed attenuation thresholds in 80–600 HU range by 40 HU increments.

Table 1. Comparisons and Correlations between Percentages of CT Right Pulmonary Vascular Volumes Quantified with Fixed Attenuation Thresholds and Nuclear Medicine Right Lung Perfusion Percentages

Fixed Threshold (HU)	80	120	160	200	240	280	320*	360*	400*	440	480	520	560	600
CT right pulmonary vascular volume percentage (%)	65.8 ± 13.8	66.1 ± 14.1	66.5 ± 14.5	67.1 ± 14.9	67.6 ± 15.4	67.9 ± 15.9	68.4 ± 16.5	69.3 ± 17.0	70.0 ± 17.2	70.4 ± 16.9	69.6 ± 18.9	68.7 ± 21.0	69.3 ± 24.6	69.8 ± 26.0
p-value of paired *t* test	< 0.001	< 0.001	< 0.003	< 0.02	> 0.06	> 0.1	> 0.4	> 0.7	> 0.2	> 0.2	> 0.5	> 0.8	> 0.6	> 0.6
Pearson correlation coefficient	0.93	0.93	0.93	0.93	0.93	0.93	0.93	0.93	0.93	0.90	0.80	0.69	0.63	0.48
Mean absolute difference (%)	5.4	5.3	5.0	4.8	4.6	4.6	4.7	4.6	4.9	5.6	9.1	12.7	17.9	22.1

*Optimal thresholds for CT pulmonary vascular volume ratio showing smallest mean absolute difference (≤ 5.0%), lowest level of statistically significant difference compared to reference values measured by lung perfusion scintigraphy, and highest Pearson correlation coefficient. HU = Hounsfield units

https://doi.org/10.3348/kjr.2019.0789

Korean Journal of Radiology
KJR

Table 2. Comparisons and Correlations between Percentages of CT Right Pulmonary Vascular Volumes Quantified with Adaptive Attenuation Thresholds and Nuclear Medicine Right Lung Perfusion Percentages

Adaptive Threshold	PA_{avg}/2.50	PA_{avg}/2.00	PA_{avg}/1.75*	PA_{avg}/1.63*	PA_{avg}/1.50*	PA_{avg}/1.25
CT right pulmonary vascular volume percentage (%)	67.2 ± 14.8	68.0 ± 15.3	68.7 ± 15.9	69.3 ± 16.2	69.7 ± 16.6	71.1 ± 17.2
p-value of paired *t* test	< 0.03	> 0.2	> 0.6	> 0.8	> 0.5	> 0.05
Pearson correlation coefficient	0.92	0.92	0.91	0.91	0.91	0.91
Mean absolute difference (%)	4.9	4.7	4.8	4.9	5.0	5.5

*Optimal thresholds for CT pulmonary vascular volume ratio showing smallest mean absolute difference (≤ 5.0%), lowest level of statistically significant difference compared to reference values measured by lung perfusion scintigraphy, and highest Pearson correlation coefficient; PA_{avg}/2.50 PA_{avg} divided by 2.50, PA_{avg}/2.00 PA_{avg} divided by 2.00, PA_{avg}/1.75 PA_{avg} divided by 1.75, PA_{avg}/1.63 PA_{avg} divided by 1.63, PA_{avg}/1.50 PA_{avg} divided by 1.50, PA_{avg}/1.25 PA_{avg} divided by 1.25. PA_{avg} = average pulmonary artery enhancement

Table 3. Comparisons between Optimal Attenuation Thresholds from This Study and Visually Determined Thresholds from Previous Study (5)

Attenuation Threshold	Fixed (320 HU)	Fixed (360 HU)	Fixed (400 HU)	Adaptive (PA_{avg}/1.75)	Adaptive (PA_{avg}/1.63)	Adaptive (PA_{avg}/1.50)	Visually-Determined (120–160 HU) (5)
CT right pulmonary vascular volume percentage (%)	68.4 ± 16.5	69.3 ± 17.0	70.0 ± 17.2	68.7 ± 15.9	69.3 ± 16.2	69.7 ± 16.6	66.3 ± 14.0
p-value of paired *t* test	> 0.4	> 0.7	> 0.2	> 0.6	> 0.8	> 0.5	0.001
Pearson correlation coefficient	0.93	0.93	0.93	0.91	0.91	0.91	0.92
Mean absolute difference (%)	4.7	4.6	4.9	4.8	4.9	5.0	5.2

PA_{avg}/1.75 PA_{avg} divided by 1.75, PA_{avg}/1.63 PA_{avg} divided by 1.63, PA_{avg}/1.50 PA_{avg} divided by 1.50.

CT pulmonary vascular volume ratio.

The calculated ratios of CT pulmonary vascular volumes were comparable between optimal fixed and adaptive attenuation thresholds, and were superior to those published in a previous study with visually determined attenuation thresholds (120–160 HU) (5) (Table 3).

DISCUSSION

In this study, we determined optimal attenuation thresholds for quantifying CT pulmonary vascular volume ratios. Our results demonstrated comparable outcomes for fixed and adaptive optimal thresholds. On average, the optimal adaptive thresholds corresponded to approximately 303 HU for PA_{avg}/1.75, 325 HU for PA_{avg}/1.63, and 353 HU for PA_{avg}/1.50. In fact, the mean attenuation values for optimal adaptive thresholds were in the same range (320–400 HU) for optimal fixed attenuation thresholds. Therefore, higher attenuation thresholds than those visually assessed in a previous study (120–160 HU) (5) should be used to obtain more accurate CT pulmonary vascular volume ratios. We previously theorized that pulmonary microcirculation including capillaries, arterioles, and venules demonstrating relatively lower attenuation values, might contribute significantly to high-fidelity pulmonary vascular volume ratios. However, based on the results of this study, we concluded that excluding enhancing soft tissue around the pulmonary vasculature from pulmonary vascular volume quantification might be crucial for obtaining more accurate ratios of CT pulmonary vascular volumes. Although there were no patients with lung atelectasis showing a high degree of contrast enhancement in this study population, higher attenuation thresholds may exclude atelectasis more effectively from pulmonary vessels.

As previously mentioned, this study demonstrated that the optimal adaptive thresholds proportional to PA_{avg} provided comparable results to optimal fixed thresholds. Theoretically, the optimal adaptive threshold is presumed superior to the optimal fixed threshold, as demonstrated in a previous study with contrast-enhanced cardiac CT (14). Despite the comparable results, we plan to apply optimal adaptive attenuation thresholds to quantify CT pulmonary vascular volume ratios in future clinical studies, when considering the wide range (250.1–956.6 HU) of PA_{avg} observed in this study.

There were no significant differences between the

 https://doi.org/10.3348/kjr.2019.0789

percentages of CT right pulmonary vascular volumes quantified with optimal thresholds and nuclear medicine right lung perfusion percentages. It is noteworthy that a small difference may result from the fundamental methodological discrepancy in quantifying the corresponding ratios between cardiothoracic CT and lung perfusion scintigraphy; i.e. pulmonary venous volumes were included in the former but not in the latter. In cyanotic congenital heart disease, the increase in systemic-pulmonary collateral arterial flow—which contributes to the pulmonary venous volumes—tends to be proportional to reduced pulmonary arterial flow (24). The difference between the two methods may be reduced when pulmonary arterial and venous volumes measured with cardiothoracic CT are separately quantified. However, such meticulous separation between pulmonary arteries and veins is one of the most technically challenging segmentation tasks, even with the assistance of a sophisticated algorithm (25).

Notably, cardiothoracic CT can provide not only pulmonary artery morphology but also differential pulmonary vascular volume ratios without additional radiation exposure to the patient. Its clinical usefulness in monitoring the effectiveness of pulmonary artery angioplasty was recently reported (7). The capability to provide CT pulmonary vascular volume ratio may expand the clinical role of cardiothoracic CT, particularly with respect to functional or quantitative evaluations, such as ventricular volumetry (26), and myocardial delayed enhancement (27). Additionally, the CT pulmonary vascular volume ratio could become a fundamental thoracic imaging method for assessing the functional aspects of various pulmonary diseases (28). For example, a central-to-peripheral pulmonary vascular volume ratio measured with CT may be used to evaluate the presence and severity of pulmonary arterial hypertension.

This study has several limitations. First, cardiothoracic CT and lung perfusion scintigraphy were performed on different days in most patients. Therefore, a change in right-to-left pulmonary vascularity ratio might have occurred during the elapsed time interval. The limitation stemming from the retrospective design of this study warrants a future prospective study. Second, a statistical comparison was not carried out to determine the optimal attenuation threshold in this study, since the differences between different thresholds were not enough to predict statistical significance. Therefore, optimal attenuation thresholds were descriptively defined to have the highest correlation, no statistically significant difference, and a mean absolute difference ≤ 5.0%, with reference values measured using lung perfusion scintigraphy.

In conclusion, the optimal fixed and adaptive thresholds for quantifying CT pulmonary vascular volume ratios appear equally useful. Considering the wide range of PA_{avg}, the application of optimal adaptive, rather than fixed thresholds may be more suitable in actual clinical practice.

Conflicts of Interest

The authors have no potential conflicts of interest to disclose.

ORCID iD

Hyun Woo Goo
https://orcid.org/0000-0001-6861-5958

REFERENCES

1. Hayabuchi Y, Mori K, Kitagawa T, Inoue M, Kagami S. Accurate quantification of pulmonary artery diameter in patients with cyanotic congenital heart disease using multidetector-row computed tomography. *Am Heart J* 2007;154:783-788
2. Shi K, Yang ZG, Xu HY, Zhao SX, Liu X, Guo YK. Dual-source computed tomography for evaluating pulmonary artery in pediatric patients with cyanotic congenital heart disease: comparison with transthoracic echocardiography. *Eur J Radiol* 2016;85:187-192
3. Pruckmayer M, Zacherl S, Salzer-Muhar U, Schlemmer M, Leitha T. Scintigraphic assessment of pulmonary and whole-body blood flow patterns after surgical intervention in congenital heart disease. *J Nucl Med* 1999;40:1477-1483
4. Sabiniewicz R, Romanowicz G, Bandurski T, Chojnicki M, Alszewicz-Baranowska J, Ereciński J, et al. Lung perfusion scintigraphy in the diagnosis of peripheral pulmonary stenosis in patients after repair of Fallot tetralogy. *Nucl Med Rev Cent East Eur* 2002;5:11-13
5. Goo HW, Park SH. Pulmonary vascular volume ratio measured by cardiac computed tomography in children and young adults with congenital heart disease: comparison with lung perfusion scintigraphy. *Pediatr Radiol* 2017;47:1580-1587
6. Goo HW. Computed tomography pulmonary vascular volume ratio in children and young adults with congenital heart disease: the effect of cardiac phase. *Pediatr Radiol* 2018;48:915-922
7. Goo HW. Computed tomography pulmonary vascular volume ratio can be used to evaluate the effectiveness of pulmonary angioplasty in peripheral pulmonary artery stenosis. *Korean J Radiol* 2019;20:1422-1430
8. Koch K, Oellig F, Oberholzer K, Bender P, Kunz P, Mildenberger P, et al. Assessment of right ventricular function by 16-detector-row CT: comparison with magnetic resonance imaging. *Eur*

https://doi.org/10.3348/kjr.2019.0789

Radiol 2005;15:312-318
9. Goo HW, Yang DH, Hong SJ, Yu J, Kim BJ, Seo JB, et al. Xenon ventilation CT using dual-source and dual-energy technique in children with bronchiolitis obliterans: correlation of xenon and CT density values with pulmonary function test results. *Pediatr Radiol* 2010;40:1490-1497
10. Goo HW, Park SH. Semiautomatic three-dimensional CT ventricular volumetry in patients with congenital heart disease: agreement between two methods with different user interaction. *Int J Cardiovasc Imaging* 2015;31:223-232
11. Scholten ET, Jacobs C, van Ginneken B, van Riel S, Vliegenthart R, Oudkerk M, et al. Detection and quantification of the solid component in pulmonary subsolid nodules by semiautomatic segmentation. *Eur Radiol* 2015;25:488-496
12. Yanagawa N, Kawata N, Matsuura Y, Sugiura T, Suzuki T, Kasai H, et al. Effect of threshold on the correlation between airflow obstruction and low attenuation volume in smokers assessed by inspiratory and expiratory MDCT. *Acta Radiol* 2015;56:438-446
13. Lee SM, Seo JB, Lee SM, Kim N, Oh SY, Oh YM. Optimal threshold of subtraction method for quantification of air-trapping on coregistered CT in COPD patients. *Eur Radiol* 2016;26:2184-2192
14. Bettinger N, Khalique OK, Krepp JM, Hamid NB, Bae DJ, Pulerwitz TC, et al. Practical determination of aortic valve calcium volume score on contrast-enhanced computed tomography prior to transcatheter aortic valve replacement and impact on paravalvular regurgitation: elucidating optimal threshold cutoffs. *J Cardiovasc Comput Tomogr* 2017;11:302-308
15. Goo HW, Allmendinger T. Combined electrocardiography- and respiratory-triggered CT of the lung to reduce respiratory misregistration artifacts between imaging slabs in free-breathing children: initial experience. *Korean J Radiol* 2017;18:860-866
16. Goo HW. Combined prospectively electrocardiography- and respiratory-triggered sequential cardiac computed tomography in free-breathing children: success rate and image quality. *Pediatr Radiol* 2018;48:923-931
17. Goo HW, Suh DS. Tube current reduction in pediatric non-ECG-gated heart CT by combined tube current modulation. *Pediatr Radiol* 2006;36:344-351
18. Goo HW. State-of-the-art CT imaging techniques for congenital heart disease. *Korean J Radiol* 2010;11:4-18
19. Goo HW. Individualized volume CT dose index determined by cross-sectional area and mean density of the body to achieve uniform image noise of contrast-enhanced pediatric chest CT obtained at variable kV levels and with combined tube current modulation. *Pediatr Radiol* 2011;41:839-847
20. Tricarico F, Hlavacek AM, Schoepf UJ, Ebersberger U, Nance JW Jr, Vliegenthart R, et al. Cardiovascular CT angiography in neonates and children: image quality and potential for radiation dose reduction with iterative image reconstruction techniques. *Eur Radiol* 2013;23:1306-1315
21. Goo HW. Is it better to enter a volume CT dose index value before or after scan range adjustment for radiation dose optimization of pediatric cardiothoracic CT with tube current modulation? *Korean J Radiol* 2018;19:692-703
22. Goo HW. Comparison of chest pain protocols for electrocardiography-gated dual-source cardiothoracic CT in children and adults: the effect of tube current saturation on radiation dose reduction. *Korean J Radiol* 2018;19:23-31
23. Hong SH, Goo HW, Maeda E, Choo KS, Tsai IC; Asian Society of Cardiovascular Imaging Congenital Heart Disease Study Group. User-friendly vendor-specific guideline for pediatric cardiothoracic computed tomography provided by the Asian Society of Cardiovascular Imaging Congenital Heart Disease Study Group: part 1. Imaging techniques. *Korean J Radiol* 2019;20:190-204
24. Goo HW. Haemodynamic findings on cardiac CT in children with congenital heart disease. *Pediatr Radiol* 2011;41:250-261
25. Park S, Lee SM, Kim N, Seo JB, Shin H. Automatic reconstruction of the arterial and venous trees on volumetric chest CT. *Med Phys* 2013;40:071906
26. Goo HW. Semiautomatic three-dimensional threshold-based cardiac computed tomography ventricular volumetry in repaired tetralogy of Fallot: comparison with cardiac magnetic resonance imaging. *Korean J Radiol* 2019;20:102-113
27. Goo HW. Myocardial delayed-enhancement CT: initial experience in children and young adults. *Pediatr Radiol* 2017;47:1452-1462
28. Goo HW. Advanced functional thoracic imaging in children: from basic concepts to clinical applications. *Pediatr Radiol* 2013;43:262-268

 https://doi.org/10.3348/kjr.2019.0789